Significance of Arrhenius activation energy in flow and heat transfer of tangent hyperbolic fluid with zero mass flux condition

K. Ganesh Kumar[1] · Abeer Baslem[2] · B. C. Prasannakumara[3] · Jihen Majdoubi[4] · Mohammad Rahimi-Gorji[5] · S. Nadeem[6,7]

Abstract
The current endeavor scrutinizes the flow of tangent hyperbolic fluid over a moving stretched surface. The characteristics of heat transfer are conferred by utilizing nonlinear radiation. Further features of mass transfer are characterized with activation energy. The problem is modeled in terms boundary layer equations by implementing the relative laws. The independent variables in the governing equations through suitable transformations are reduced which are further tackled numerically via RKF-45 technique. Several physical parameters are varied in order to evaluate the behaviors of velocity, temperature and concentration distributions. It is established that higher values of We parameter increases the velocity profile. Further it is obtained that rate of heat transfer enhances as N_r parameter increases.

List of symbols

b	Stretching rate
C_f	Skin friction
c_p	Specific heat
C	Nanoparticle volume fraction
D_B	Brownian diffusion coefficient
D_T	Thermophoresis diffusion coefficient
E	Activation energy
k	Thermal conductivity (W/mK)
k^*	Mean absorption coefficient (W/mK)
Nb	Brownian motion parameter
Nt	Thermophoresis parameter
Nu	Local Nusselt number
Nr	Radiation parameter
Pr	Prandtl number
Sc	Schmidt number
Sh_x	Local Sherwood number
T	Temperature of the fluid (K)
T_w	Temperature at the wall (K)
T_∞	Ambient fluid temperature (K)
u,v	Velocity components along x and y Directions (ms^{-1})
u_w	Stretching sheet velocity (W/mK)
x	Coordinate along the stretching Sheet (m)
y	Distance normal to the stretching sheet (m)

✉ S. Nadeem
sohail.nadeem@tdtu.edu.vn

K. Ganesh Kumar
ganikganesh@gmail.com

Abeer Baslem
a.baslem@mu.edu.sa

Jihen Majdoubi
j.majdoubi@mu.edu.sa

Mohammad Rahimi-Gorji
mohammad.rahimigorji@ugent.be; m69.rahimi@yahoo.com

1. Department of Mathematics, SJM Institute of Technology, Chitradurga, Karnataka 577502, India

2. Department of Business Management, College of Science and Humanities at AlGhat, Majmaah University, P.O. Box 66, Majmaah 11952, Kingdom of Saudi Arabia

3. Department of PG Studies and Research in Mathematics, Davanagere University, Davanagere, Karnataka, India

4. Department of Computer Science, College of Science and Humanities at Alghat, Majmaah University, Al-Majmaah 11952, Saudi Arabia

5. Faculty of Medicine and Health Science, Ghent University, 9000 Ghent, Belgium

6. Mathematics and its Applications in Life Sciences Research Group, Ton Duc Thang University, Ho Chi Minh City, Vietnam

7. Faculty of Mathematics and Statistics, Ton Duc Thang University, Ho Chi Minh City, Vietnam

Greek symbols

v Kinematic viscosity
ϕ Rescaled nanoparticle volume fraction
ρ Density of the base fluid (kg/m^3)
σ Reaction rate
δ Temperature difference
κ Boltzmann constant
θ Dimensionless temperature
η Similarity variable
α Thermal diffusivity

1 Introduction

The motion of heat for a viscous fluid has numerous industrialized, biomedical and engineering demands for instance capacity generator, petroleum productions, plasma research, cancer therapy, the laminar boundary layer dominance in aerodynamics and numerous others. But this concept takes a long journey to shape up for this position. In 1904, Prandtl suggested the laminar boundary layer theory which humor that the viscous impact would be limited to thin shear surfaces adjacent borders in the case of the flow of fluids with very small viscosity (Schlichting et al. 1960). Sakiadis (1961a b) has studied the boundary layer Blasius motion due to surface supplying with constant speed from a slit into a liquid at relaxes. Crane (1970) has investigated the flow over a stretching sheet. Numerous researchers for instance Dutta et al. (1985), Char (1988), Gupta and Gupta (1977) expanded the research of Crane (1970). Varied features of such problems have been studied by different researchers for instance Hayat et al. (2008). Hayat et al. (2006), Xu and Liao (2005) and Cortell (2005, 2006).Motion past a cylinder is assumed to be 2-D boundary layer flow across a stretching cylinder was invoked by Datta et al. (2006). Elbarbary was analyzed by heat transfer effects on micropolar across a stretching cylinder (Elbarbary and Elgazery 2005). Wang (1988) has investigated the steady two dimensional flow of a fluid across a stretching cylinder. Ishak et al. (2008) have studied the MHD motion and transfer of heat past a stretching cylinder. Ishak et al. (2008) have numerical investigation on the effect of suction/blowing on the motion across a stretching cylinder. Butt et al. (2016) have explored Heat transfer effects on hydromagnetic entropy generation flow over a horizontal stretching cylinder. They are obtaining solutions by using bvp4c technique in MATLAB.

Radiation plays very important role in engineering, industry, and humankind also. In human kinds radiation is used for medicines, excavation, radiology lab, MRI scans

etc. Akinshilo (2019) was scrutinized the flow of hydromagnetic fluid flow across vertical micro channel with radiation effects, in this paper they are obtaining solution by implementing Runge–Kutta scheme. A steady 3D non-linear radiation on flow of a carreau fluid across a bidirectional stretching sheet was studied by Khan et al. (2018). They concluded that by escalating values of Hartmann number the velocity profile is declines and opposite behaviour is seen in temperature profile. Khan et al. (2018) was deliberated by impact of linear radiation on third grade fluid for coating analysis. In this paper they are obtaining solution by using HAM. Hashim et al. (Hamid et al. 2018) studied by heat and mass transfer effects on non-Newtonian fluid over a circular cylinder.

Magnetohydrodynamic plays a key role in industry, engineering, heat transfers etc. Hydromagnetics is the revise of the magnetic premises of electrically conducting fluid. There are several applications in magneto hydrodynamics they are cosmology, seismology, metal detectors etc.Heat transfer effects on hydromagnetic nano fluid by using Buongiorno's model were analyzed by Ajam et al. (2018).they are obtaining solution by using OHAM. Durga Prasad et al. (2018) was scrutinized by analytical approximation on MHD nano fluid across a semi-infinite plate. Khan et al. (2018) was invoked by homogenious –hetrogenious reactions on hydromagnetic non-newtonian fluid across a cylinder. Siti et al. (2018) was investigated by MHD flow past a stretching disk. Heat and fluid flow along a stretching cylinder was studied by Vikas et al. (2018). In this paper they are presenting graphical presentations along with stability analysis. Ismail et al. (2019) analyzed the study of stability analysis on an unsteady hydromagnetic flow across a shrinking sheet. Gholinia et al. (2019) was analyzed by heat and mass transfer effects on hydromagnetic nano fluid across a stretching sheet. In this paper they are presenting graphical representations by using Runge–Kutta method. Heat transfer effects on hydromagnetic natural convection in Darcy-Forchhimer were scrutinized by Sajjadi et al. (2019).

In modern days the abnormal trend of nanofluid is due to its unexpected thermal properties and have dynamic role in heat transfer enhancement of material processing and industrial thermal managements. Free convection flows permanently faced in engineering tools and nuclear reactor technology. Prasannakumara et al. (Prasannakumara et al. 2017) deliberate effort on radiative heat transfer of nanofluids using magnetic field over a plate. They perceive that the Nusselt number and Sherwood number are enhanced for nonlinear stretching sheet. Kumar et al. (2018) represented the Marangoni effects on nanofluid in the presence of heat. Recently various researchers studied heat transfer of nanofluids (Kumar et al. 2018; Kumar and Chamkha 2019; Kumar 2019; Usman et al. 2018; Anwar

and Rasheed 2017; Mebarek-Oudina 2019; Mebarek-Oudina 2017; Raza et al. 2019; Gourari et al. 2019; Verma and Sinha 2015; Verma et al. 2017; Ganesh et al. 2020; Nadeem et al. 2020; Rashid et al. 2020; Abbas et al. 2020; Kahshan et al. 2019; Uddin et al. 2019; Akermi et al. 2019; Ganesh Kumar et al. 2019).

The above literature analysis discloses that no work occurs on incompressible tangent hyperbolic nanoliquid flow past a permeable surface. The combined effect of magnetic field and nanofluid across a permeable surface are accounted. By using similarity transformations PDE'S can be transformed into ODE'S and explained numerically. Outcomes are represented through graphs for the parameters of concern.

2 Mathematical formulation

Here firstly assume that flow is steady and the incompressible tangent hyperbolic nanoliquid flow past a permeable surface is considered. The flow occupies to $y > 0$, velocity of the sheet is $u_w(x) = bx, b > 0$ and further x-axis taken along the sheet (Fig. 1).

The constitutive equation of tangent hyperbolic fluid is,

$$\bar{\tau} = \left[\mu_0 + (\mu_0 + \mu_\infty) \tanh\left(\Gamma\bar{\gamma}\right)^n \right]\bar{\gamma}, \tag{a}$$

in which, $\bar{\tau}$ is the extra stress tensor, μ_∞ the infinite shear rate viscosity, μ_0 the zero shear rate viscosity, Γ is the time dependent material constant, n the power law index i.e. flow behavior index and $\bar{\gamma}$ is defined as,

$$\bar{\gamma} = \frac{1}{2}\sqrt{\frac{1}{2}\sum_i\sum_j\bar{\gamma}_{ij}\bar{\gamma}_{ji}} = \sqrt{\frac{1}{2}\Pi}. \tag{b}$$

Consider the equation (a), for the case when $\mu_\infty = 0$ because it is not possible to discuss the problem for the infinite shear rate viscosity and since we are considering tangent hyperbolic fluid that describing shear thinning effects so $\Gamma\bar{\gamma} < 1$. Then equation (a) will takes the form,

$$\bar{\tau} = \mu_0\left[\left(\Gamma\bar{\gamma}\right)^n\right]$$
$$\bar{\tau} = \mu_0[1 + n(\Gamma\bar{\gamma} - 1)]\bar{\gamma}. \tag{c}$$

Governing equations for tangent hyperbolic fluid model after applying the boundary layer approximations can be defined as Abdul Maleque (2013), Dhlaminia et al. (2019), Kumar et al. (2017),

$$\frac{\partial u}{\partial x} + \frac{\partial v}{\partial y} = 0 \tag{1}$$

$$u\frac{\partial u}{\partial x} + v\frac{\partial u}{\partial y} = v(1-n)\frac{\partial^2 u}{\partial y^2} + \sqrt{2}vn\Gamma\left(\frac{\partial u}{\partial y}\right)\frac{\partial^2 u}{\partial y^2} - \frac{\sigma B_0^2}{\rho}u, \tag{2}$$
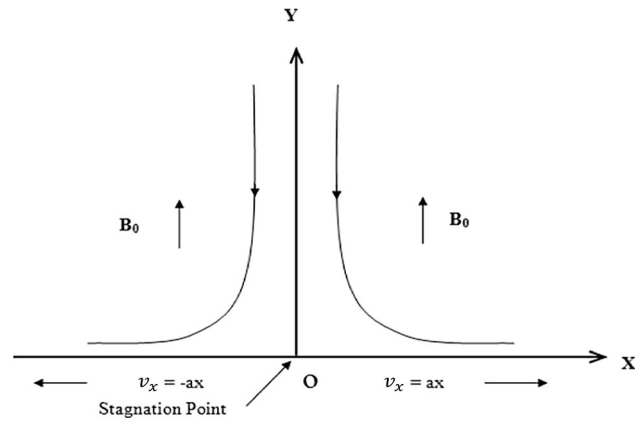

Fig. 1 Physical model and coordinate system

$$u\frac{\partial T}{\partial x} + v\frac{\partial T}{\partial y} = \alpha\left(\frac{\partial^2 T}{\partial y^2}\right)$$
$$+ \tau\left\{D_B\left(\frac{\partial C}{\partial y}\frac{\partial T}{\partial y}\right) + \left(\frac{D_T}{T_\infty}\right)\left[\left(\frac{\partial T}{\partial y}\right)^2\right]\right\}$$
$$- \frac{1}{\rho C_p}\frac{\partial q_r}{\partial y}, \tag{3}$$

$$u\frac{\partial C}{\partial x} + v\frac{\partial C}{\partial y} = D_B\frac{\partial^2 C}{\partial y^2} + \left(\frac{D_T}{T_\infty}\right)\left(\frac{\partial^2 T}{\partial y^2}\right) - k_r^2(C$$
$$- C_\infty)\left(\frac{T}{T_\infty}\right)^m\exp\left(\frac{-Ea}{\kappa T}\right) \tag{4}$$

The following imposed conditions of the model are;

$$u = u_w(x), v = v_w, T$$
$$= T_w, \ D_B\frac{\partial C}{\partial y} + \frac{D_T}{T_\infty}\frac{\partial T}{\partial y} = 0 \text{ (passive control of } \phi) \text{ at } y$$
$$= 0$$

$$u \to 0, T \to T_\infty, C \to C_\infty \ as \ y \to \infty \tag{5}$$

Here $v_w > 0$ notes as injection, $v_w < 0$ noted as suction. The third term on RHS of Eq. (5) denotes modified Arrhenius formula in which k_r^2 for rate of reaction, Ea for activation energy, κ for Boltzmann constant and m dimensionless fitted rate constant which lies in the range $-1 < m < 1$.

Implementation Rosseland approximation q_r defined as,

$$q_r = -\frac{4\sigma^*}{3k^*}\frac{\partial T^4}{\partial y} = \frac{16\sigma^*}{3k^*}T^3\frac{\partial T}{\partial y}, \tag{6}$$

use of (6) in (3), we get;

$$u\frac{\partial T}{\partial x} + v\frac{\partial T}{\partial y} = \frac{\partial}{\partial y}\left[\left(\alpha + \frac{16\sigma^*}{3k^*}T^3\frac{\partial T}{\partial y}\right)\frac{\partial T}{\partial y}\right]$$
$$+ \tau\left\{D_B\left(\frac{\partial C}{\partial y}\frac{\partial T}{\partial y}\right) + \left(\frac{D_T}{T_\infty}\right)\left[\left(\frac{\partial T}{\partial y}\right)^2\right]\right\}, \tag{7}$$

To obtain the similarity result use the following variables

$$\eta = \left(\frac{u_w}{vx}\right)^{1/2} y, \ f(\eta) = \frac{\psi}{(xvu_w)^{1/2}}, \ \theta(\eta) = \frac{T - T_\infty}{T_w - T_\infty}, \ \phi(\eta)$$

$$= \frac{C - C_\infty}{C_\infty} (\text{passive control of } \phi)$$

(8)

where $T = T_\infty(1 + (\theta_w - 1)\theta(\eta))$ and $\theta_w = {}^{T_w}\!/_{T_\infty}, \theta_w > 1$ being temperature ration parameter.

Applying (8) in (1, 2, 4 and 7), one can have;

$$(1 - n)f'''(\eta) - [f'(\eta)]^2 + f''(\eta)f(\eta)$$
$$+ nW_e f''^2(\eta)f'''(\eta) - Mf'(\eta)$$
$$= 0,$$

(9)

$$\left([(1 + Nr(\theta_w - 1))\theta]^3 \theta'\right)' + \Pr\left(f\theta' + Nb\theta'\phi' + Nt\theta'^2\right)$$
$$= 0,$$

(10)

$$\phi'' + Scf\phi' + \frac{Nt}{Nb}\theta'' - Sc\sigma(1 + \delta\theta)^m \phi \exp\left(\frac{-E}{1 + \delta\theta}\right) = 0,$$

(11)

COresponding boundary conditions are;

$$f(0) = S, f'(0) = 1, \theta(0) = 1, Nb\phi'(0) + Nt\theta'(0)$$
$$= 0(\text{passive control of } \phi), f'(\infty) \to 0, \theta(\infty)$$
$$\to 0, \phi(\infty) \to 0.$$

(12)

The dimentionless numbers in Eqs. (9–12) are $\lambda = \lambda_2^2 a^2$ for material parameter, $Nr\left(= \frac{16\sigma^* T_\infty^3}{3kk^*}\right)$ for radiation parameter, $Nb\left(= \frac{\tau D_B C_\infty}{v}\right)$ for Brownian movement. $Nt\left(= \frac{\tau D_T(T_f - T_\infty)}{vT_\infty}\right)$ for thermophoretic, $\Pr\left(= \frac{v}{\alpha}\right)$ for Prandtl number, $Sc\left(= \frac{v}{D_B}\right)$ for Schmidt number, $\sigma\left(= \frac{k_r^2}{b}\right)$ for reaction rate, $\delta\left(= \frac{T_f - T_\infty}{T_\infty}\right)$ for temperature difference, $E\left(= \frac{Ea}{\kappa T_\infty}\right)$ for activation energy, $W_e = \frac{\sqrt{2b}\Gamma u_w}{\sqrt{v}}$ is the Weissenberg number and n is the power law index parameter and $S = -\frac{v_w}{\sqrt{bv}}$ for mass transfer parameter.

The physical quantities of interest like skin friction coefficient (C_f) and local Nusselt number (Nu_x), and Sherwood number are defined as,

$$c_f = \frac{\tau_w}{\rho u_w^2}, Nu_x = \frac{u_w q_w}{bk(T_\infty - T_w)} \quad \text{and}$$
$$Sh_x = \frac{u_w q_m}{aD_b(C_w - C_\infty)},$$

(13)

where τ_w is known as shear stress along the wall, q_w is known as heat flux, q_m is nano particle mass flux,

$$\tau_w = \mu_0\left((1 - n)\frac{\partial u}{\partial y} + \frac{n\Gamma}{\sqrt{2}}\left(\frac{\partial u}{\partial y}\right)^2\right), \quad q_w = -k\frac{\partial T}{\partial y}|_{y=0}$$

$$\text{and} \quad q_m = -D\frac{\partial C}{\partial y}|_{y=0}.$$

(14)

Finally the expression of drag friction (C_f), local Nusselt number (Nu) and Sherwood number (Sh) written as,

$$\sqrt{Re}C_f = \left[(1 - n)f''(\eta) + \frac{n}{2}W_e(f''(\eta))^2\right]_{\eta=0}, Nu Re_x^{-1/2}$$

$$= -\left(1 + Nr\theta_w^3\right)\theta'(0) \text{ and}$$

$$Sh Re_x^{-1/2} = \frac{Nt}{Nb}\theta'(0)(\text{passive control of } \phi)$$

(15)

where $Re_x = {}^{u_w x}\!/_v$ for local Reynolds number.

3 Numerical method

The dimensionless arrangement of Eqs. (9)–(11) with the conditions (12) are profoundly coupled differential conditions. One needs to turn towards numerical strategies to acquire the arrangement of such conditions. In this investigation, we have utilized the method Runge–Kutta–Fehlberg fourth–fifth order with shooting system. The calculations have been done utilizing the representative programming Maple.

The algorithm of Runge–Kutta–Fehlberg –forth- fifth order method is given by;

$$k_0 = F(\bar{x}_m, \bar{y}_m),$$

$$k_1 = F\left(\bar{x}_m + \frac{h}{4}, \bar{y}_m + \frac{hk_0}{4}\right),$$

$$k_2 = F\left(\bar{x}_m + \frac{3}{8}h, \bar{y}_m + \left(\frac{3}{32}k_0 + \frac{9}{32}k_1\right)h\right),$$

$$k_3 = F\left(\bar{x}_m + \frac{12}{13}h, \bar{y}_m + \left(\frac{1932}{2197}k_0 - \frac{7200}{2197}k_1 + \frac{7296}{2197}k_2\right)h\right),$$

$$k_4 = F\left(\bar{x}_m + h, \bar{y}_m + \left(\frac{439}{216}k_0 - 8k_1 + \frac{3860}{513}k_2 - \frac{845}{4104}k_3\right)h\right),$$

$$k_5 = F\left(\bar{x}_m + \frac{h}{2}, \bar{y}_m + \left(-\frac{8}{27}k_0 + 2k_1 - \frac{3544}{2565}k_2 + \frac{1859}{4104}k_3 - \frac{11}{40}k_4\right)h\right),$$

$$\bar{y}_{m+1} = \bar{y}_m + h\left(\frac{25}{216}k_0 + \frac{1408}{2565}k_2 + \frac{2197}{4109}k_3 - \frac{1}{5}k_4\right),$$

$$\bar{y}_{m+1} = \bar{y}_m + h\left(\frac{16}{135}k_0 + \frac{6656}{12825}k_2 + \frac{28561}{56430}k_3 - \frac{9}{50}k_4 + \frac{2}{55}k_5\right),$$

4 Results and discussion

The flawless perception of the physical problem is discussed in this section. The prominent characteristics of the impact of a combination of nanofluids on velocity,

temperature and concentration augmentation are evaluated through graphical representation of numerical data and tables. Figures 2, 3, 4, 5, 6, 7, 8, 9, 10, 11, 12, 13, 14, 15, 16, 17, 18 represent the fluid flow, temperature and concentration profiles. For this computation we choose the parameter values $Nb = Nt = 0.3, Nr = 3, Pr = 3, n = 0.5, W_e = 0.8, \theta_w = 1.2, \sigma = \delta = E = 1$ and $Sc = 0.5$.

Figure 2 captured the impact of M on velocity profiles against similarity variable η respectively. We perceived from Fig. 2 that by enhancing magnetic number M the fluid flow diminished progressively. Because the Lorentz force is an opposite force for strengthen magnetic number which resists the liquid motion. The influence of Weissenberg parameter W_e can be seen in Fig. 3. From these figures show that the velocity profile enhances with boost up values of W_e. Furthermore, the thickness of hydrodynamic boundary layer is high for rising values of W_e.

The behaviour of Radiation parameter Nr is illustrated in Fig. 4 An increase in Radiation parameter Nr shows the significant enhancement in the fluid temperature function. Physically speaking, by strengthening Nr yields more heat into the liquid, as a consequence the thickness of associated the energy boundary layer enhanced. Thus, Nr effects plays a key role in magnify the rate of heat transfer.

The influence of temperature ratio parameter θ_w on $\theta(\eta)$ is illustrated in Fig. 5. The temperature and species profiles rises by improving values of θ_w thickness of boundary layer increased. From Figs. 6, 7 illustrates that for escalating values of δ and E concentration profile declines for δ and opposite behaviour is seen in E.

From Fig. 8 shows that for boost up values of Schmidt number Sc concentration decreases for both the phases. Physically, enhancing values of Schmidt number Sc the mass diffusivity declines. Figures 9 and 10 are demonstrates the influence of Nt and Nb on $\theta(\eta)$. It shows that an
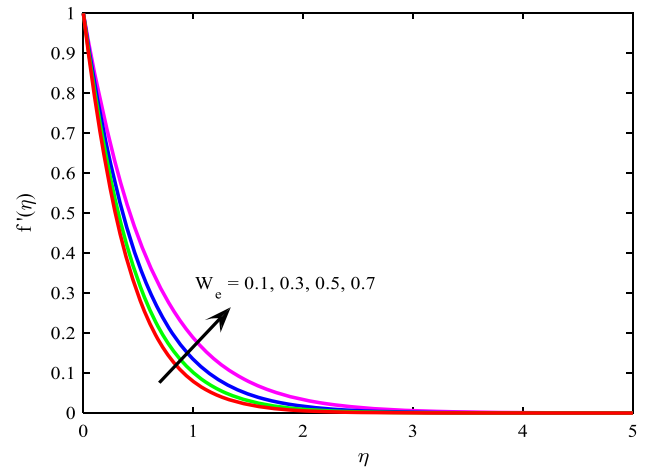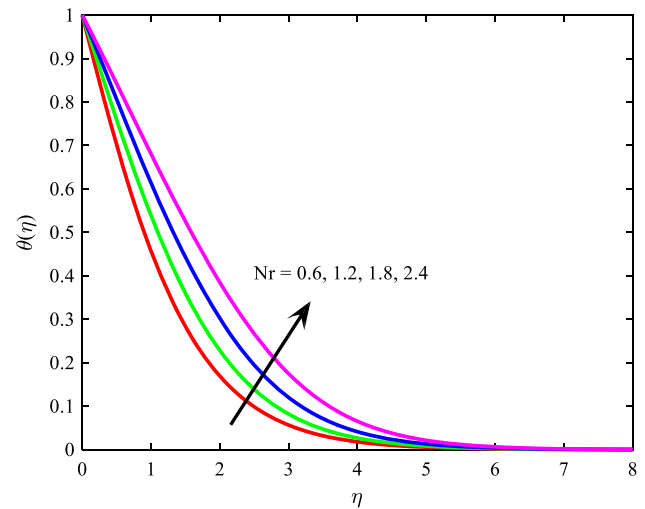

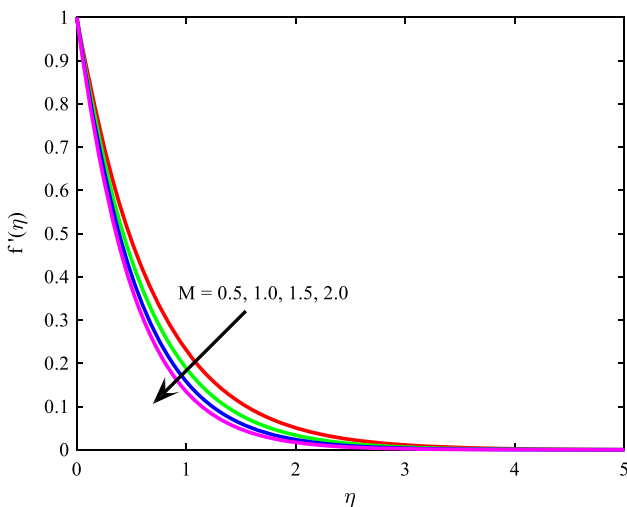**Fig. 3** Impact of W_e on $f'(\eta)$

Fig. 4 Impact of N_r on $\theta(\eta)$

Fig. 2 Impact of M on $f'(\eta)$

Fig. 5 Impact of θ_w on $\theta(\eta)$

Fig. 6 Impact of δ on $\phi(\eta)$
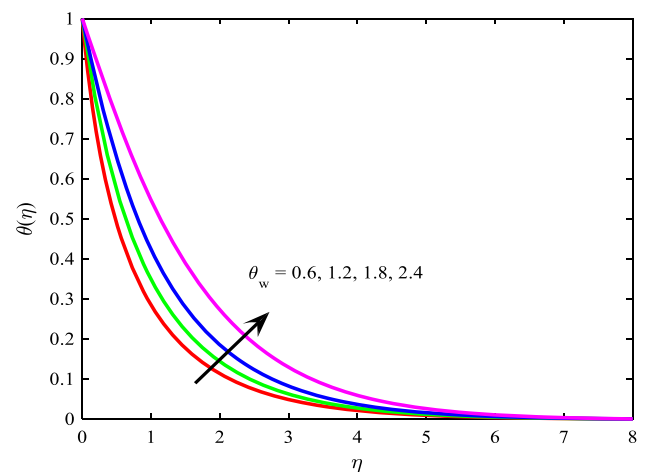
Fig. 7 Impact of E on $\phi(\eta)$
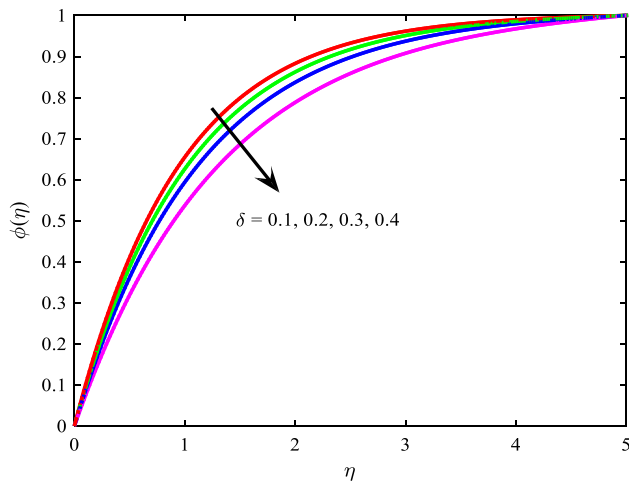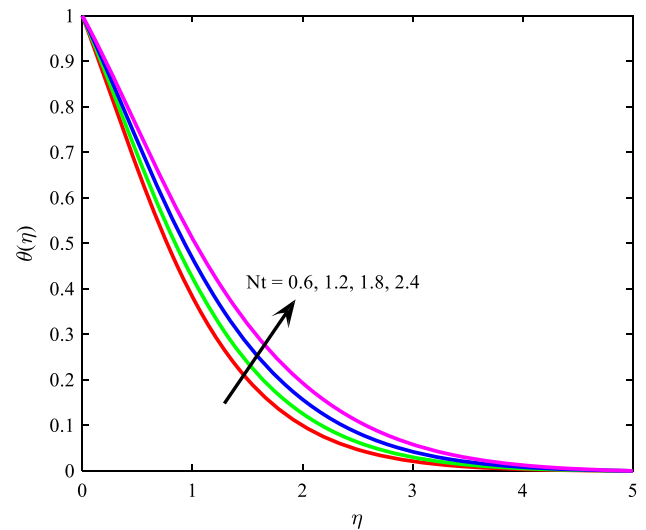
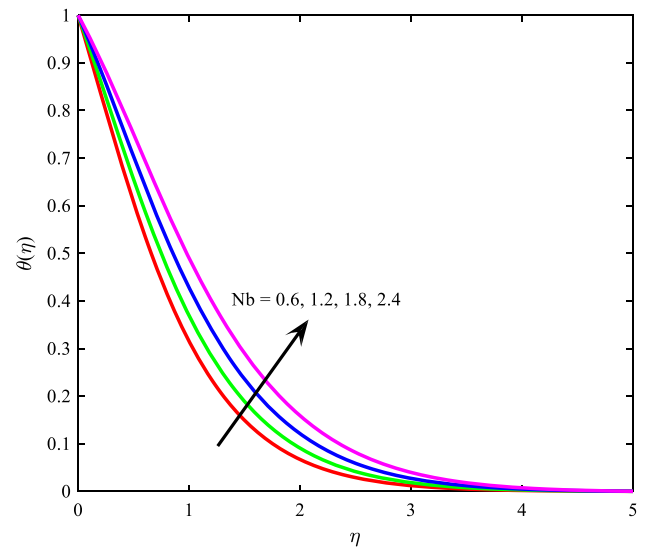**Fig. 8** Impact of Sc on $\phi(\eta)$

Fig. 9 Impact of Nt on $\theta(\eta)$
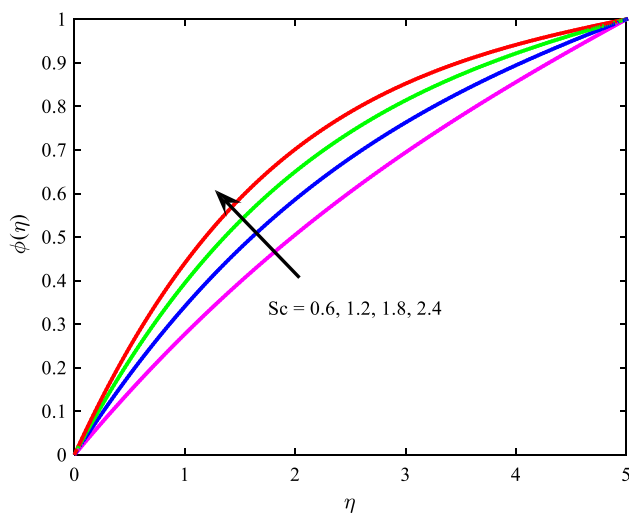

Fig. 10 Impact of Nb on $\theta(\eta)$

increase in Nt and Nb enhances the $\theta(\eta)$ and hence, the associated thickness of the boundary layer also enhances.

Figure 11 elucidates the effect of Nb on ϕ field. A reduction in ϕ field is obtained for the larger values of Nb parameter. Correspondingly thickness of boundary layer exhibits the same behavior as that of nanoparticle concentration profile. This is because of the larger Brownian motion of the suspended particle, due to its increment in its corresponding parameter.

In the boundary layer region Nt plays a vital role on the ϕ field. This effect is captured in Fig. 12. From this figure it is clear that for gradually increasing values of Nt concentration profile is increased. Physically, the thermophoretic is a force that one particle exerts on the other particle. Due to which the particles in the hotter region are
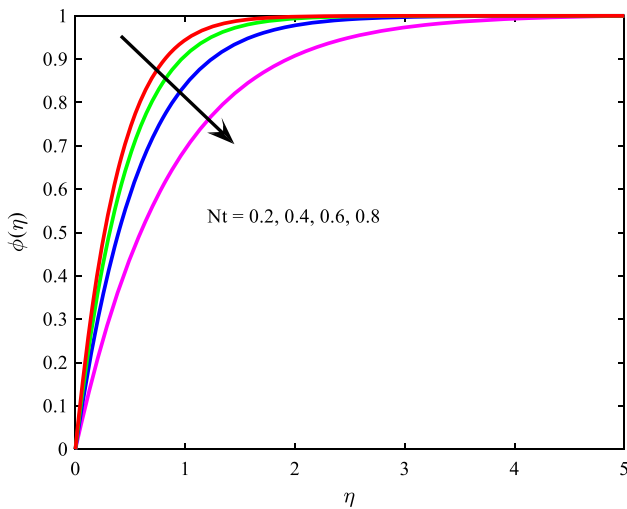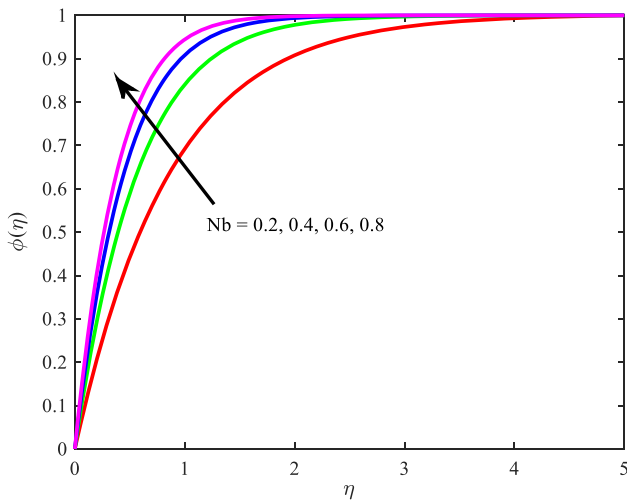
Fig. 11 Impact of Nt on $\phi(\eta)$
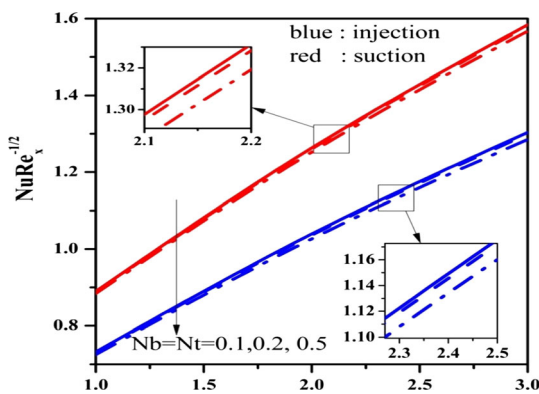

Fig. 12 Impact of Nb on $\phi(\eta)$

Fig. 13 Influence of Nb and Nt on $-NuRe_x^{-\frac{1}{2}}$

Fig. 14 Influence of Sc and E on $-ShRe_x^{-\frac{1}{2}}$

Fig. 15 Stream lines for when $M = 0.5$

moved to the colder region. As a result an acclivity in the concentration is noted. The effects of Nb and Nt on $-NuRe_x^{-\frac{1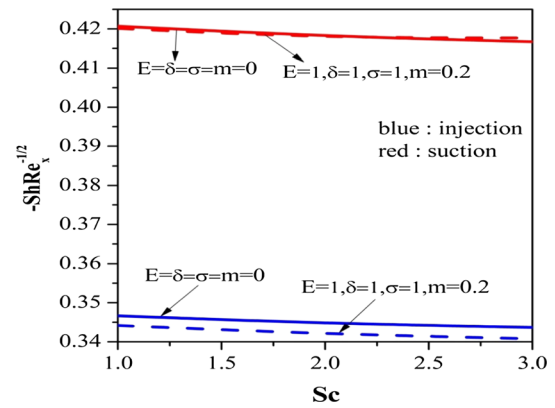}{2}}$ is established in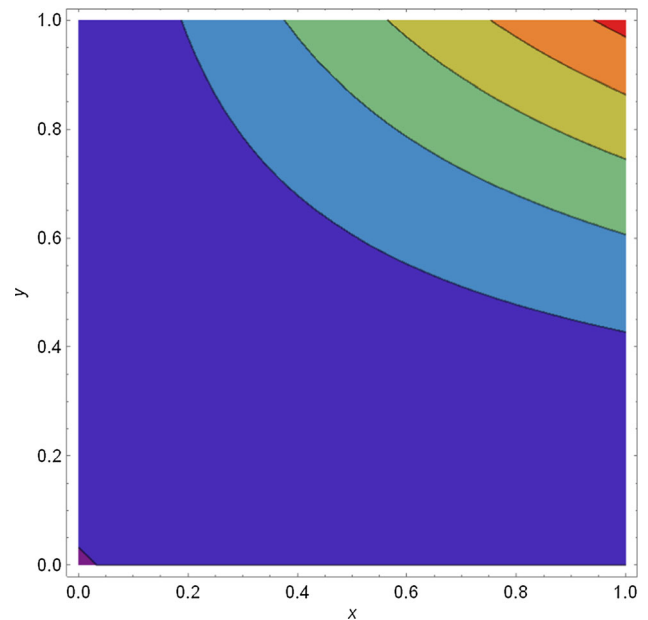 Fig. 13. It shows that the $-NuRe_x^{-\frac{1}{2}}$ decreases for both injection and suction case for large values of Nb and Nt. Figure 14 IS prepared to establish the influence of Sc verses E on $-ShRe_x^{-\frac{1}{2}}$. It is clear that, $-ShRe_x^{-\frac{1}{2}}$ decays for enlarged values of Sc verses E.

Finally, to get a clear view of the flow field patterns, the stream line dynamics are reported in Figs. 15, 16, 17 and 18 for with peculiar values of Magnetic parameter M and Weissenberg number W_e For Magnetic parameter M and Weissenberg number W_e is strengthened, the fluid particle traces a definite curve along x-direction where the surface is present. But it is clear that the there is a retardation in the flow pattern.
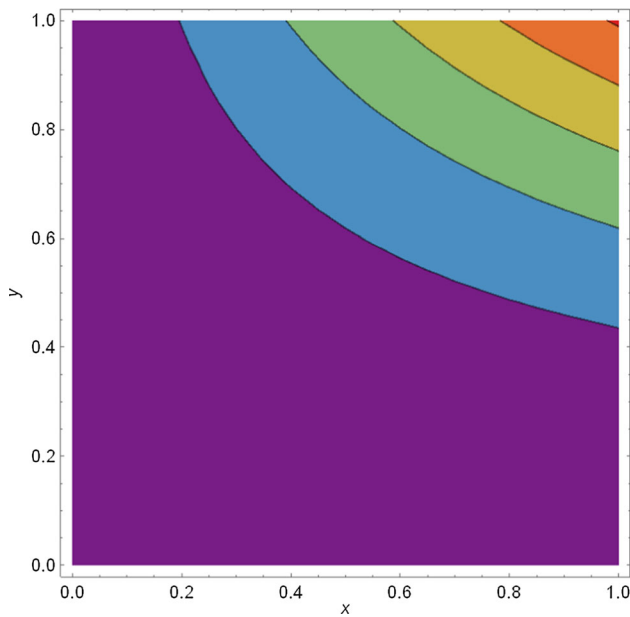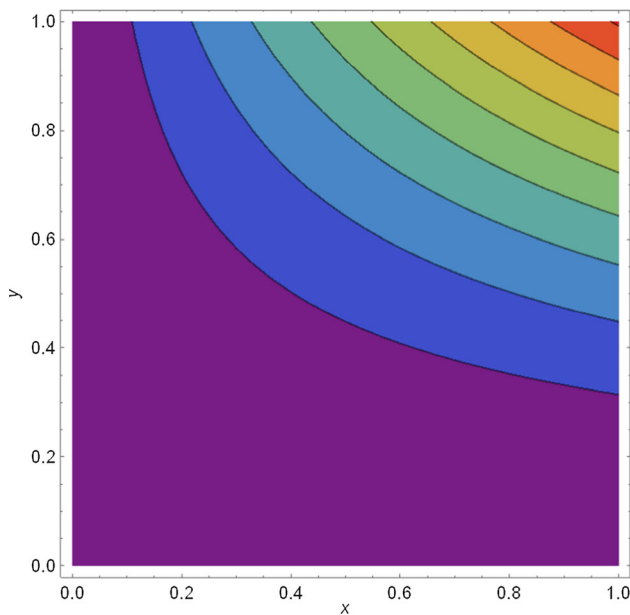
Fig. 16 Stream lines for when $M = 2.0$

Fig. 18 Stream lines for when $W_e = 1.0$

- Both concentration and temperature profiles enhance for increasing values of Nb parameter.
- Temperature and velocity profiles shows reverse trend in rising values of Nt.
- Momentum boundary layer thickness decreases for rising values of M.
- The concentration profile and corresponding boundary layer thickness decreases for enhancing values of δ and E.
- Higher Nr plays a key role in magnify the rate of heat transfer. This is because, higher Nr enhances the temperature profile and also enhances the corresponding boundary layer thickness.

Fig. 17 Stream lines for when $W_e = 0.1$

5 Conclusion

Fully developed steady of flow and heat transfer of tangent hyperbolic nanofluid fluid over a stretching sheet is considered. In this paper the effect of zero mass flux, activation energy and impact of applied magnetic field is taken into consideration. The outcome of the present work is as follows:

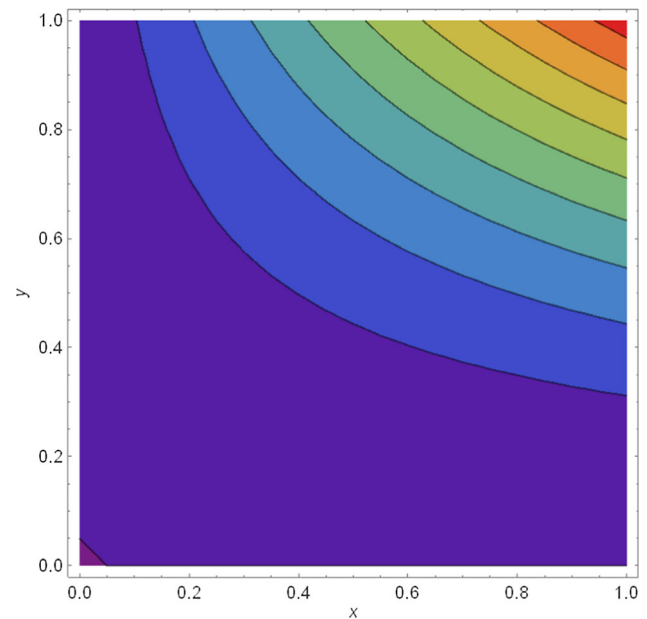- Velocity of the fluid increases as W_e parameter increases.

References

Abbas N, Nadeem S, Malik MY (2020) Theoretical study of micropolar hybrid nanofluid over Riga channel with slip conditions. Phys A

Abdul Maleque K (2013) Effects of binary chemical reaction and activation energy on MHD boundary layer heat and mass transfer flow with viscous dissipation and heat generation/absorption. ISRN Thermodyn. https://doi.org/10.1155/2013/284637

Ajam H, Sajad Jafari S, Freidoonimehr N (2018) Analytical approximation of MHD nano-fluid flow induced by a stretching permeable surface using Buongiorno's model. Ain Shams Eng J 9(4):525–536

Akermi M, Jaballah N, Alarifi I, Rahimi-Gorji M, Chaabane R, Ouada H, Majdoub M (2019) Synthesis and characterization of a novel hydride polymer P-DSBT/ZnO nano-composite for optoelectronic applications. J Mol Liq 287:110963

Akinshilo AT (2019) Mixed convective heat transfer analysis of MHD fluid flowing through an electrically conducting and non-

conducting walls of a vertical micro-channel considering radiation effect. Appl Therm Eng 156:506–513

Anwar MS, Rasheed A (2017) Heat transfer at microscopic level in a MHD fractional inertial flow confined between non-isothermal boundaries. Eur Phys J Plus 132:305–322

Butt AS, Ali A, Mehmood A (2016) Numerical investigation of magnetic field effects on entropy generation in viscous flow over a stretching cylinder embedded in a porous medium. Energy 99:237–249

Char MI (1988) Heat transfer of a continuous, stretching surface with suction or blowing. J Math Anal Appl 135(2):568–580

Cortell R (2005) Flow and heat transfer of a fluid through a porous medium over a stretching surface with internal heat generation/absorption and suction/blowing. Fluid Dyn Res 37(4):231–245

Cortell R (2006) Effects of viscous dissipation and work done by deformation on the MHD flow and heat transfer of a viscoelastic fluid over a stretching sheet. Phys Lett A 357(4):298–305

Crane LJ (1970) Flow past a stretching plate. Zeitschriftfürangewandte Mathematik und Physik (ZAMP) 21(4):645–647

Datta P, Anilkumar D, Roy S, Mahanti NC (2006) Effect of non-uniform slot injection (suction) on a forced flow over a slender cylinder. Int J Heat Mass Transf 49(13):2366–2371

Dhlaminia M, Kameswaran PK, Sibanda P, Motsaa S, Mondal H (2019) Activation energy and binary chemical reaction effects in mixed convective nanofluid flow with convective boundary conditions. J Comput Des Eng 6(2):149–158

Durga Prasad P, Kiran Kumar RVMSS, Varma SVK (2018) Heat and mass transfer analysis for the MHD flow of nanofluid with radiation absorption. Ain Shams Eng J 9:801–813

Dutta BK, Roy P, Gupta AS (1985) Temperature field in flow over a stretching sheet with uniform heat flux. Int Commun Heat Mass Transfer 12(1):89–94

Elbarbary EME, Elgazery NS (2005) Flow and heat transfer of a micropolar fluid in an axi-symmetric stagnation flow on a cylinder with variable properties and suction (numerical study). Acta Mech 176(3–4):213–229

Ganesh Kumar K, Rahimi-Gorji M, Gnaneswara Reddy M, Chamkha AJ, Alarifi IM (2019) Enhancement of heat transfer in a convergent/divergent channel by using carbon nanotubes in the presence of a Darcy-Forchheimer medium. Microsyst Technol. https://doi.org/10.1007/s00542-019-04489-x

Ganesh G, Sinha S, Verma T (2020) Numerical simulation for optimization of the indoor environment of an occupied office building using double-panel and ventilation radiator. J Build Eng 29:101139

Gholinia M, Hoseini E, Gholinia S (2019) A numerical investigation of free convection MHD flow of Walters-B nanofluid over an inclined stretching sheet under the impact of Joule heating. Thermal Sci Eng Prog 11:272–282

Gourari S, Mebarek-Oudina F, Hussein A, Kolsi L, Hassen W, Younis O (2019) Numerical study of natural convection between two coaxial inclined cylinders. Int J Heat Tech 37(3):779–786

Gupta PS, Gupta AS (1977) Heat and mass transfer on a stretching sheet with suction or blowing. Can J Chem Eng 55(6):744–746

Hamid HA, Khan M, Khan U (2018) Thermal radiation effects on Williamson fluid flow due to an expanding/contracting cylinder with nanomaterials: dual solutions. Phys Lett A 382(30):1982–1991

Hayat T, Abbas Z, Sajid M (2006) Series solution for the upper-convected Maxwell fluid over a porous stretching plate. Phys Lett A 358(5):396–403

Hayat T, Javed T, Abbas Z (2008) Slip flow and heat transfer of a second grade fluid past a stretching sheet through a porous space. Int J Heat Mass Transf 51(17):4528–4534

Ishak A, Nazar R, Pop I (2008a) Magnetohydrodynamic (MHD) flow and heat transfer due to a stretching cylinder. Energy Convers Manag 49(11):3265–3269

Ishak A, Nazar R, Pop I (2008b) Uniform suction/blowing effect on flow and heat transfer due to a stretching cylinder. Appl Math Model 32(10):2059–2066

Ismail N, Arifin N, Nazar R, Bachok N (2019) Stability analysis of unsteady MHD stagnation point flow and heat transfer over a shrinking sheet in the presence of viscous dissipation. Chin J Phys 57:116–126

Kahshan M, Dianchen L, Rahimi-Gorji M (2019) Hydrodynamical study of flow in a permeable channel: application to flat plate dialyzer. Int J Hydrogen Energy 44(31):17041–17047

Khan M, Hashim HS (2018) Heat generation/absorption and thermal radiation impacts on three-dimensional flow of Carreau fluid with convective heat transfer. Journal of Molecular Liquids 272:474–480

Khan Z, Shah RA, Altaf M, Kha A (2018a) Effect of thermal radiation and MHD on non-Newtonian third grade fluid in wire coating analysis with temperature dependent viscosity. Alexand Eng J 57(3):2101–2112

Khan M, Ullah S, Malik MY, Hussain A (2018b) Numerical analysis of MHD Carreau fluid flow over a stretching cylinder with homogenous-heterogeneous reactions. Result Phys 9:1141–1147

Kumar KG (2019) Exploration of flow and heat transfer of non-Newtonian nanofluid over a stretching sheet by considering slip factor. Int J Numer Meth Heat Fluid Flow. https://doi.org/10.1108/HFF-11-2018-0687

Kumar KG, Chamkha AJ (2019) Darcy-Forchheimer flow and heat transfer of water-based Cu nanoparticles in convergent/divergent channel subjected to particle shape effect. Eur Phys J Plus 134(3):107

Kumar KG, Gireesha BJ, Krishanamurthy MR, Rudraswamy NG (2017) An unsteady squeezed flow of a tangent hyperbolic fluid over a sensor surface in the presence of variable thermal conductivity. Result Phys 7:3031–3036

Kumar KG, Gireesha BJ, Krishnamurthy MR, Prasannakumara BC (2018a) Impact of convective condition on Margoni convection flow and heat transfer in Casson nanofluid with uniform heat source sink. Journal of Nanofluids 7:108–114

Kumar KG, Ramesh GK, Gireesha BJ, Gorla RSR (2018b) Characteristics of joule heating and viscous dissipation on three-dimensional flow of Oldroyd B nanofluid with thermal radiation. Alexand Eng J 57(3):2139–2149

Mebarek-Oudina F (2017) Numerical modeling of the hydrodynamic stability in vertical annulus with heat source of different lengths. Eng Sci Technol Int J 20(4):1324–1333

Mebarek-Oudina F (2019) Convective heat transfer of Titania nanofluids of different base fluids in cylindrical annulus with discrete heat source. Heat Transfer: Asian Res. 48:135–147

Nadeem S, Abbas N, Malik MY (2020) Inspection of hybrid based nanofluid flow over a curved surface. Comput Methods Programs Biomed 189:105193

Prasannakumara BC, Gireesha BJ, Krishnamurthy MR, Ganesh Kumar K (2017) MHD flow and nonlinear radiative heat transfer of Sisko nanofluid over a nonlinear stretching sheet. Inf Med Unlock 9:123–132

Rashid M, Ansar K, Nadeem S (2020) Effects of induced magnetic field for peristaltic flow of Williamson fluid in a curved channel. Statistical Mechanics and its Applications, Physica A, p 123979

Raza J, Mebarek-Oudina F, Chamkha AJ (2019) Magnetohydrodynamic flow of molybdenum disulfide nanofluid in a channel with shape effects. Multidisc Model Mater Struct 15(4):737–757

Sajjadi H, Amiri Delouei A, Izadi M, Mohebbi R (2019) Investigation of MHD natural convection in a porous media by double MRT

lattice Boltzmann method utilizing MWCNT–Fe$_3$O$_4$/water hybrid nanofluid. Int J Heat Mass Transf 132:1087–1104

Sakiadis BC (1961a) Boundary layer behavior on continuous solid surfaces: I. Boundary layer equations for two dimensional and axi-symmetric flow. AIChE J 7(1):26–28

Sakiadis BC (1961b) Boundary layer behavior on continuous solid surfaces: II. The boundary layer on a continuous flat surface. AIChE J 7(2):221–225

Schlichting H, Gersten K, Krause E, Oertel H (1960) Boundary-layer theory, vol 7. McGraw-Hill, New York

Soid SK, Ishak A, Pop I (2018) MHD flow and heat transfer over a radially stretching/shrinking disk. Chin J Phys 56:58–66

Uddin S, Mohamad M, Rahimi-Gorji M, Roslan R, Alarifi IM (2019) Fractional electro-magneto transport of blood modeled with magnetic particles in cylindrical tube without singular kernel. Microsyst Technol. https://doi.org/10.1007/s00542-019-04494-0

Usman M, Haq RU, Hamid M, Wang W (2018) Least square of heat transfer of water based *Cu* and *Ag* nanoparticles along a converging/diverging channel. J Mol Liq 249:856–867

Verma T, Sinha S (2015) Numerical simulation of contaminant control in multi-patient intensive care unit of hospital using computational fluid dynamics. J Med Imaging Health Inf 5(5):1088–1092

Verma TN, Sahu AK, Sinha SL (2017) Study of particle dispersion on one bed hospital using computational fluid dynamics. Mater Proc 4(9):10074–10079

Vikas P, Singh P, Yadav AK (2018) Stability analysis of MHD outer velocity flow on a stretching cylinder. Alexand Eng J 57:2077–2083

Wang CY (1988) Fluid flow due to a stretching cylinder. Phys Fluids 31:466–468

Xu H, Liao SJ (2005) Analytic solutions of magnetohydrodynamic flows of non- Newtonian fluids caused by an impulsively stretching plate. J Non-Newton Fluid Mech 159:46–55